Pergamon

Tetrahedron 58 (2002) 621–628

TETRAHEDRON

Competitive indicator methods for the analysis of citrate using colorimetric assays

Shawn C. McCleskey, Axel Metzger, Chris S. Simmons and Eric V. Anslyn*

Department of Chemistry and Biochemistry, University of Texas at Austin, Austin, TX 78712, USA

Received 15 June 2001; revised 25 August 2001; accepted 26 August 2001

Abstract—A competitive indicator method for studying host–guest complexes is extended to systems forming I:H, I:H_2, and A:H complexes of indicator (I), host (H) and competing analyte (A). Methods are applied to complexes of a synthetic organic host (**1**) with commercially available indicators xylenol orange (**4**) and methylthymol blue (**5**). Utilizing complexometric indicators results in an observable shift in λ_{max} upon binding of the analyte and, subsequently may enhance the sensitivity of these competition assays due to a larger dynamic range in the change of absorption. The binding constants for the association between **4** and **1** are $K_1=7.05\times10^3\ M^{-1}$ and $K_2=2.08\times10^3\ M^{-1}$ and between **5** and **1** the binding constants are $K_1=3.95\times10^3\ M^{-1}$ and $K_2=1.10\times10^2\ M^{-1}$. Competition assays using UV–Vis spectroscopy and each host–indicator ensemble allowed for the determination of citrate concentration in various beverages.

1. Introduction

There have been numerous reports describing advances in the rational design of synthetic receptors for selective complexation of neutral and ionic species such as sugars,[1] metal ions,[2] and anions.[3] Hence, the rational design of host molecules for the binding of small organic guests is refined to the point that their use as selective sensors is very realistic. Selectivity can be achieved through recognition of the analyte at a receptor site that is preorganized by an appropriate scaffold, and by a combination of effects such as ion-pairing, hydrogen-bonding, π-interactions and solvophobic interactions.

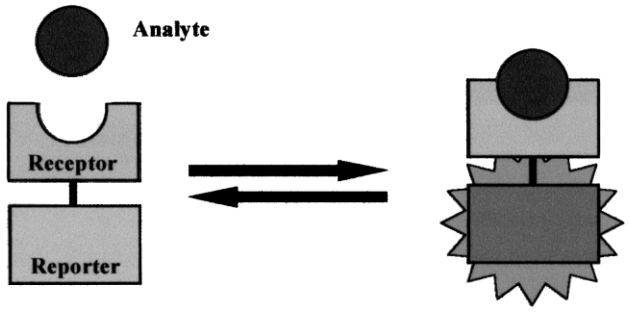

Figure 1. Molecular recognition scheme: upon binding of the analyte, a sensing element will have a detectable response.

Sensing involves the detection of a signal from a reporter molecule that is produced by a binding event (Fig. 1). When the receptor molecule interacts with an analyte, the microenvironment of a reporter molecule needs to be perturbed sufficiently to modulate the signal from the reporter, thereby detecting the presence of the analyte. This approach allows for the spectroscopic monitoring of chemical interactions. Many examples of chemosensors have been developed using the theme of covalently attaching a sensing element to a receptor.[4] A disadvantage to introducing additional covalent architecture for converting a receptor into a sensor is that this often requires more synthetic steps which can be time consuming and expensive.

A tool that has been exploited in the field of biochemistry is the use of a competition assay.[5] With this technique, an antibody is anchored to a support, which is subjected to a tagged antigen. When this sensing ensemble is exposed to a complex fluid containing the analyte of interest, the number of tagged antigens displaced can be correlated to the amount of analyte present in the sample.

Similarly, competition assays can be used as a relatively simple method for determining association constants (Fig. 2).[6] Introduction of a surrogate substrate, or indicator, to the receptor will establish an equilibrium of binding between the indicator and the receptor and a receptor–indicator complex, resulting in a particular optical response. Addition of the analyte of interest to the receptor–indicator ensemble perturbs the equilibrium. The change in the established equilibrium between the indicator and the receptor is dependent on the relative degree of association between the analyte and the receptor. This approach allows synthetic

Keywords: competition assay; indicators; UV–Vis spectroscopy; binding constants; citrate.

* Corresponding author. Tel.: +1-512-471-0068; fax: +1-512-471-7791; e-mail: anslyn@ccwf.cc.utexas.edu

0040–4020/02/$ - see front matter
PII: S0040-4020(01)01093-6

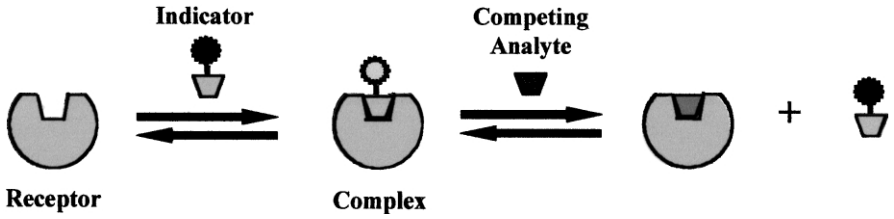

Figure 2. A competition assay allows for the presence of a competing analyte to be detected upon displacement of an indicator molecule.

receptors to act as sensors without introducing additional covalent architecture.

Our group has used this approach with a series of synthetic organic hosts in order to detect various analytes.[7–9] In one system, a receptor for citrate was developed that is selective for this tris-carboxylate compound even in the presence of other common carboxylates.[7] The choice of citrate as the target analyte was due to the potential commercial interest in a sensor for citrate by beverage bottling companies.

The receptor **1** (or host) consists of a 2,4,6-triethylbenzene core substituted with guanidinium moieties in the 1, 3, and 5 positions. Each adjacent substituent on the benzene ring alternates above and below the plane of the ring to minimize steric interactions, causing the guanidiniums to lay on one face of the benzene ring.[10] Receptors containing similar structures to **1** have demonstrated that the preorganization helps facilitate the binding of small organic guests.[7–9,11,12]

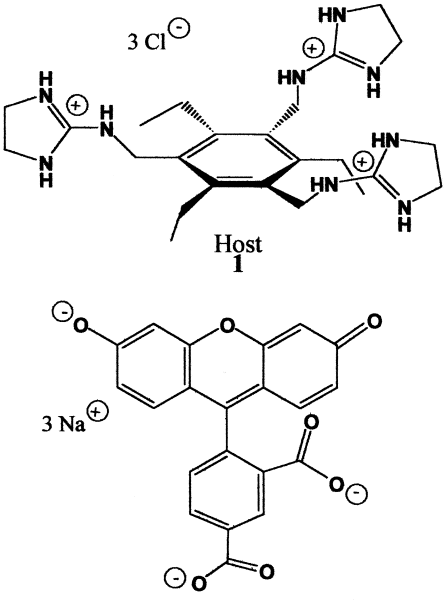

At neutral pH, citrate (**2**) is trianionic, and this charge leads to the ability to distinguish citrate from other possible interfering species. Host **1** is complementary to citrate in both charge and hydrogen-bonding ability. The use of guanidiniums was employed because their geometry is conducive for the binding of carboxylates, and they remain protonated over a wider pH range than ammonium species.[13]

The sensing properties of **1** for citrate were investigated with the use of competition assays. Initially, a sensing ensemble was created by introducing **3** (5-carboxyfluorescein) to **1**. As seen in Fig. 3A, the absorbance of **3** at pH 7.4 increases at 495 nm upon association with **1**. The observed increase in absorbance was rationalized to be a result of increased ionization of the phenol on the xanthene ring due to the positively charged microenvironment of the host molecule. The binding constant was found to be $4.7\times10^3\ M^{-1}$ under Benesi–Hildebrand[14] conditions in 25% (v/v) water in methanol at pH 7.4.

Addition of sodium citrate to the indicator–host complex causes a decrease in the observed absorbance of fluorescein at 495 nm (Fig. 3B). It was reasoned that the 5-carboxyfluorescein (**3**) was expelled from the binding pocket due to the higher binding affinity of citrate with **1**. A binding constant for citrate with **1** was found to be $2.9\times10^5\ M^{-1}$ in this solvent system. Significantly reduced affinities were found for succinate, glutarate (both valued close to $2\times10^2\ M^{-1}$) and acetate (less than $10\ M^{-1}$).[7]

A practical use of an ensemble of **1** and **3** was demonstrated by evaluating the amount of citrate in various complex mixtures. Calibration curves were generated for varying

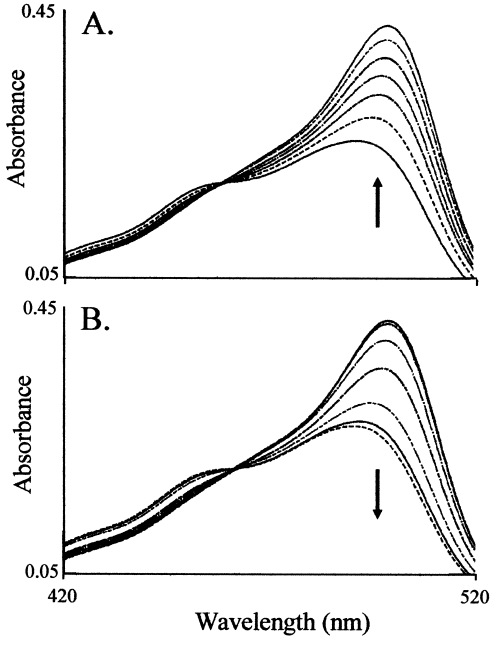

Figure 3. UV–Vis spectra of **3** in 25% (v/v) water in methanol with 5 mM HEPES buffer at pH 7.4. (A) Addition of **1** to a solution of **3** at constant concentration (14 μM) causes an increase in the absorbance. (B) Addition of **2** to the sensing ensemble **1**:**3** at constant concentration (75 μM **1**, 14 μM **3**) causes a decrease in absorbance at 495 nm.

amounts of citrate from the absorbance data obtained from the citrate competition assay. With these plots, aliquots of different citrus beverages were added to a solution of the **1**:**3** complex and the absorbance recorded.[8] This allowed for the analysis of citrate in commercially available beverages and further demonstrated that **1** possesses selectivity for citrate in the presence of other competing analytes.

Although this assay was successful, we desired two improvements. One was a λ_{max} shift, which creates a color change and therefore a larger dynamic range in the change in absorbance. The second goal was to show that many commercially available indicators could be used with the same receptor. This gives chemists a larger latitude in the ability to choose indicators for displacement assays using synthetic receptors. Herein, we summarize the new developments and describe the utility of this method in the context of the analysis of citrate in citrus beverages using a synthetic receptor paired with an optical signaling molecule.

2. Results and discussion

Using competition assays for the evaluation of analytes in solution requires that the indicator form a complex with the ligand or host molecule. Another requirement is that the absorption spectra of the complexed form differ significantly from the absorption spectra of the uncomplexed form. The choice of indicators in this study was guided by two factors. First, the binding of carboxylates with guanidinium groups imbedded in aminoimidazoline groups is well precedented,[7–9] and therefore the use of complexometric indicators possessing carboxylates in their structure were explored. Second, we chose indicators that change color as a function of pH, thereby we expect similar color changes within the microenvironment of the host. Xylenol orange (**4**) and methylthymol blue (**5**) were chosen as the indicators for the purposes of our studies.

At neutral pH, metal cations typically coordinate to the iminiodiacetic acid residues and the auxochromic phenol oxygen of **4** and **5** inducing a shift in the λ_{max}.[15] We expected that complexation of **4** or **5** to **1** would result in a similar color change of the indicator due to increased ionization of the phenols. The structural features of these two indicators (I) clearly show that there are two similar iminiodiacetic acid binding sites that can associate with host **1** (H), giving I/H and I/H_2 molecular complexes (Scheme 1).

To both explore the stoichiometry of binding and to measure the affinity constants, we first studied the associative properties of **1** with **4** and **5**. Titration experiments were conducted to determine the binding constants for each dye with host **1**. As described previously, host **1** associates with **3** in a 1:1 fashion. However, the dyes used in these studies (**4** and **5**) are expected to associate with the host giving I:H and I:H_2 complexes. This expectation is borne out by the lack of sharp isosbestic points (Figs. 4 and 5).

$$I + H \overset{K_1}{\rightleftharpoons} I{:}H$$
$$I{:}H + H \overset{K_2}{\rightleftharpoons} I{:}H_2$$
$$I{:}H_2 + A \overset{K_3}{\rightleftharpoons} A{:}H + I{:}H$$
$$I{:}H + A \overset{K_4}{\rightleftharpoons} I + A{:}H$$
$$A + H \overset{K_5}{\rightleftharpoons} A{:}H$$

Scheme 1. Equilibria for the systems studied.

The absorbance of **4** (Fig. 4A) at pH 7.5 increases at 577 nm upon association with **1**, while the absorbance decreases at 445 nm (solutions change from an orange color to a pink–red). Similarly, the absorbance of **5** (Fig. 5A) at pH 7.5 increases at 607 nm upon addition of **1** with a decrease in absorbance at 454 nm (solutions change from a light yellow to a cobalt blue). It is reasoned that the binding of the positively charged host molecule to the carboxylates on the indicator would lower the pK_a of the indicator phenol groups due to the positive microenvironment present in the host. The observed color changes correlate with the indicators acting as if they are in a more basic microenvironment. The increased ionization state of the indicators is due to the positive charges on the receptor, and the increased electron density on the auxochromic oxygen leads to the observed λ_{max} changes.

In Figs. 4A and 5A, a large change in absorbance was observed with the addition of **1** to each indicator. For instance, the percent difference in absorbance at 577 nm between the absorbance of the dye in solution and the

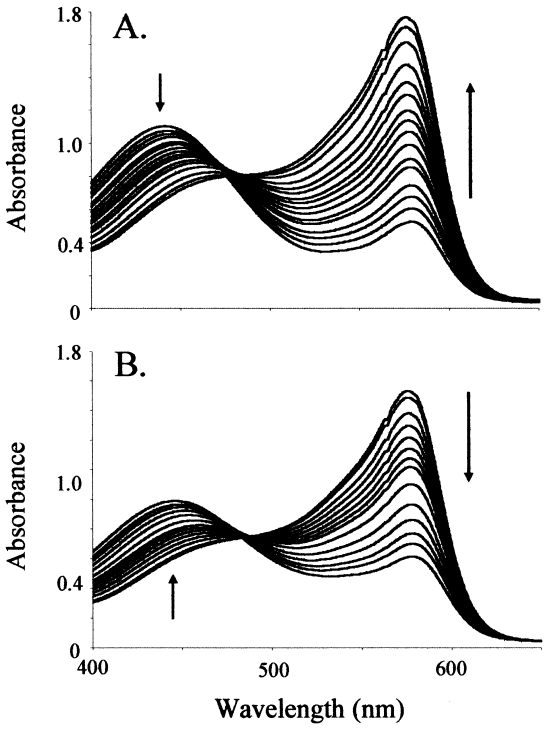

Figure 4. UV–Vis spectra of **4** in 25% (v/v) water in methanol with 10 mM HEPES buffer at pH 7.5. (A) Addition of **1** to a solution of **4** at constant concentration (55 μM) causes an increase in absorbance at 577 nm with a decrease in absorbance at 445 nm. (B) Addition of **2** to a solution of **4**:**1** at constant concentration (55 μM **4**, 1.13 mM **1**) causes a decrease in absorbance at 577 nm with a decrease in absorbance at 454 nm (arrows indicate the direction of change in the absorbance intensity).

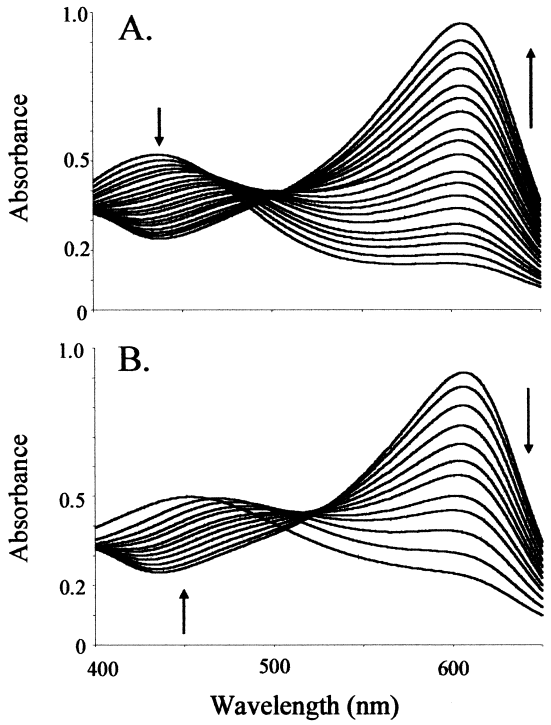

Figure 5. UV–Vis spectra of **5** in 25% (v/v) water in methanol with a 10 mM HEPES buffer at pH 7.5. (A) Addition of **1** to a solution of **5** at constant concentration (55 μM) causes an increase in absorbance at 607 nm with a decrease in absorbance at 454 nm. (B) Addition of **2** to a solution of **5**:**1** at constant concentration (55 μM **5**, 1.13 mM **1**) causes a decrease in absorbance at 607 nm with a decrease in absorbance at 454 nm (arrows indicate the direction of change in the absorbance intensity).

absorbance of the **4**:**1** complex in Fig. 4A was 238%, and the percent difference in absorbance at 607 nm in Fig. 5A was calculated to be 521%. This is a significantly larger dynamic range in change in signal compared to the 73% increase in signal observed with the addition of **1** to 5-carboxyfluorescein (Fig. 3A). The dramatic increase in signal in both cases with indicators **4** and **5** is attributed to their ability to shift their λ_{max} upon complexation with host **1**.

As shown in Figs. 4B and 5B, addition of citrate to the indicator–host complexes causes a reverse in the observed absorbance of both xylenol orange and methylthymol blue at 577 and 607 nm, respectively. As seen with the citrate assay employing 5-carboxyfluorescein, the indicator is expelled from the binding pocket due to the higher binding affinity of **1** with citrate (Scheme 2).

Extraction of the binding constants, K_1 and K_2, for the association between each indicator molecule and the host is complicated. There are four variables: two binding constants (K_1 and K_2), and two different extinction coefficients (1:1 indicator–host complex, and 1:2 indicator–host complex). A method for determining 1:1 and 1:2 binding constants from optical spectroscopy data has been discussed.[6] Further, we have discussed how NMR data can be used to analyze 1:1 and 1:2 equilibria.[16] Although the equations and methods we will discuss here have been previously published, we briefly describe our slightly modified procedure, and in Appendix A we show the derivations. Hopefully, these derivations will make this procedure more readily applicable to the work of others.

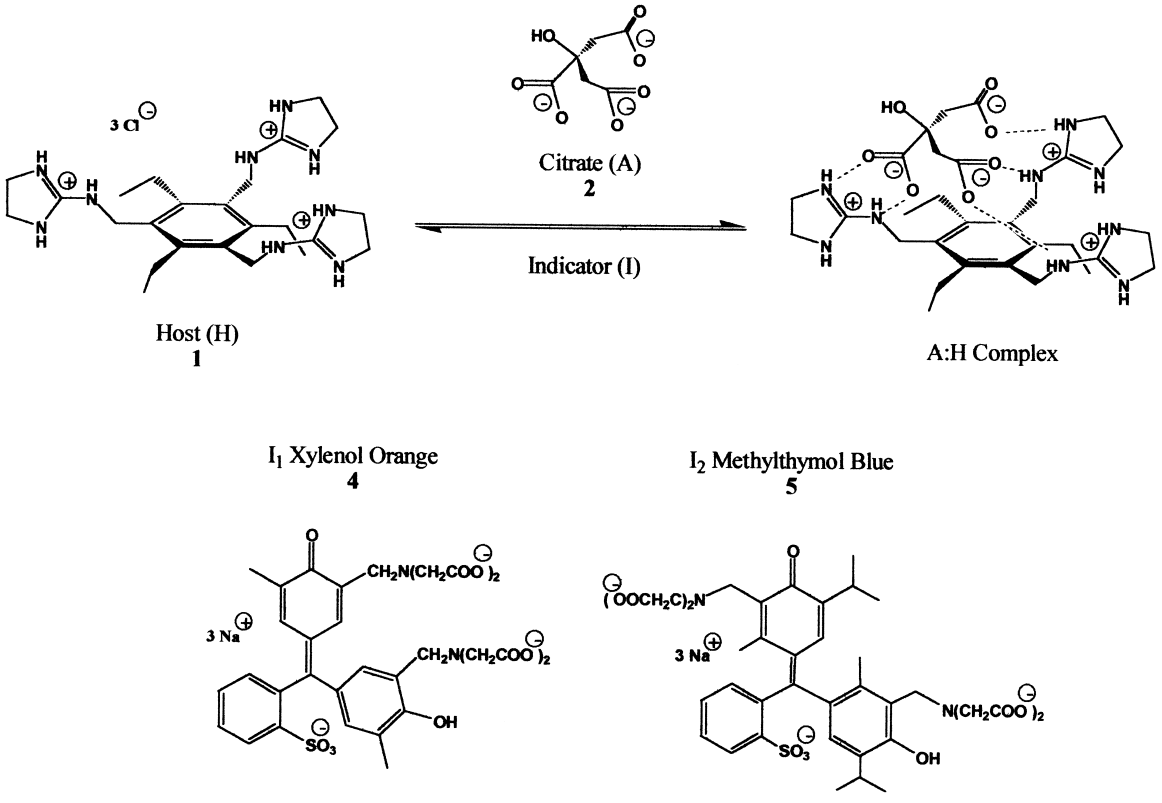

Scheme 2. The structures of the host and indicators used to sense for citrate.

Eq. (1) shows the relationship of the observed change in absorbance ($\Delta A/b$) to the concentration of the complexes in solution where $[I_T]$ are the total indicator concentration and $\Delta\epsilon_1$ and $\Delta\epsilon_2$ is the difference between the ϵ_{IH} or ϵ_{IH2} and ϵ_I extinction coefficients, respectively,

$$\frac{\Delta A}{b} = \frac{(K_1[H_i][I_T])(\Delta\epsilon_1 + \Delta\epsilon_2 K_2[H_i])}{1 + K_1[H_i] + K_2K_1[H_i]^2} \quad (1)$$

where $[H_i]$ is the concentration of host free in solution. The equilibria for this system are given by:

$$K_1 = \frac{[IH]}{[I][H]} \quad (2)$$

$$K_2 = \frac{[IH_2]}{[IH][H]} \quad (3)$$

If one solves for $[H_i]$ from Eqs. (2) and (3) as a function of total host $[H_T]$ and total indicator $[I_T]$ concentration, Eq. (4) is obtained.

$$K_1K_2[H_i]^3 + K_1(2K_2[I_T] - K_2[H_T] + 1)[H_i]^2 + (K_1[I_T] - K_1[H_T] + 1)[H_i] - [H_T] = 0 \quad (4)$$

The program Mathematica 3.0 was used to solve Eq. (4) for $[H_i]$ with multiple values of $[H_T]$ and several initial estimates of K_1, K_2, $\Delta\epsilon_1$, and $\Delta\epsilon_2$. Each value for $[H_i]$ is substituted into Eq. (1). The fit of Eq. (1) to the data is accomplished by prompting the user for initial estimates for K_1, K_2, $\Delta\epsilon_1$, and $\Delta\epsilon_2$. The model equation (Eq. (1)) is overlaid graphically with the experimental values obtained for $\Delta A/b$ (the path length is 1.00 cm) and $[H_T]$. The values K_1, K_2, $\Delta\epsilon_1$, and $\Delta\epsilon_2$ are modified and the data reploted until the best fit between experimental data and the model is visually achieved, as shown in Fig. 6.

The binding constants determined for the **4**:**1** molecular complex were $K_1=7.05\times10^3\ M^{-1}$ and $K_2=2.08\times10^3\ M^{-1}$. The affinity constants determined for the **5**:**1** molecular complex were $K_1=3.95\times10^3\ M^{-1}$ and $K_2=1.10\times10^2\ M^{-1}$. These results show that xylenol orange has a larger affinity for **1** than methylthymol blue. This observation may be attributed to the presence of the isopropyl groups on methythymol blue as opposed to the methyl groups at the corresponding positions in the xylenol orange structure. The added steric bulk on **5** could hinder access of **1** to the indicator binding sites, resulting in slightly smaller binding constant values.

The equilibrium equations given in Scheme 1 for the displacement of the indicators upon addition of **2** are as follows:

$$K_3 = \frac{[AH][IH]}{[IH_2][A]} \quad (5)$$

$$K_4 = \frac{[AH][I]}{[IH][A]} \quad (6)$$

The equilibrium expression for the association of host **1** with citrate is:

$$K_5 = \frac{[AH]}{[H][A]} \quad (7)$$

Hence, the displacement constants K_3 and K_4 can be determined by using the following relationships:

$$K_3 = \frac{K_5}{K_2} \quad (8)$$

$$K_4 = \frac{K_5}{K_1} \quad (9)$$

With xylenol orange, the values for K_3 and K_4 obtained from Eqs. (8) and (9) are 1.39×10^2 and $41.1\ M^{-1}$, respectively. In the methylthymol blue studies, the values for K_3 and K_4 obtained from Eqs. (8) and (9) are $2.64\times10^3\ M^{-1}$ and $73.4\ M^{-1}$, respectively. These values for K_3 and K_4 were calculated using the binding constant (K_5) presented earlier.[8] It was reasoned previously that the association constants for methylthymol blue to **1** were smaller than the corresponding K_1 and K_2 values for xylenol orange due to added steric bulk on the methylthymol blue structure. It follows that the displacement constants for xylenol orange upon introduction of citrate are smaller than the corresponding K_3 and K_4 values for methylthymol blue because of the stronger association of the **4**:**1** complex. The association of the **5**:**1** complex is slightly weaker than the **4**:**1** complex and therefore the **5**:**1** complex will disassociate more readily in order for the **1**:**2** complex to form upon introduction of citrate.

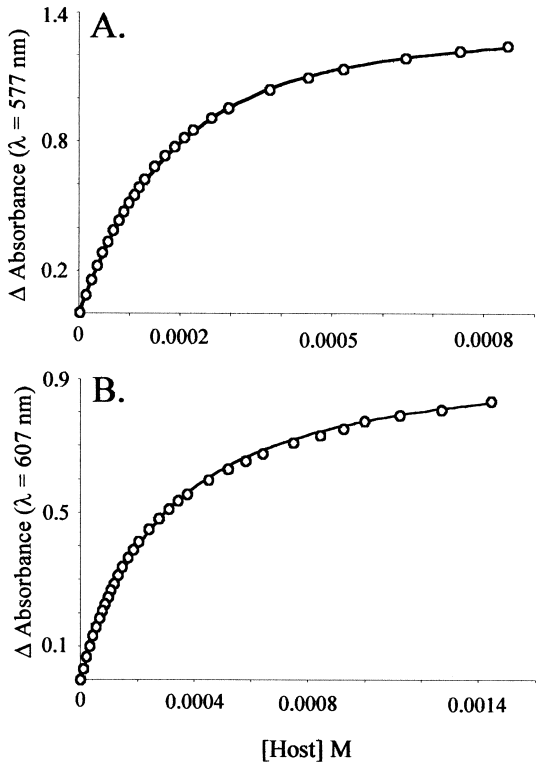

Figure 6. Theoretical fit (—) of Eq. (1) to the experimental data (○) obtained from ΔA as a function of the addition of **1** to each indicator. (A) Isotherm plot for addition of **1** to **4** (λ=577 nm). (B) Isotherm plot for the addition of **1** to **5** (λ=607 nm).

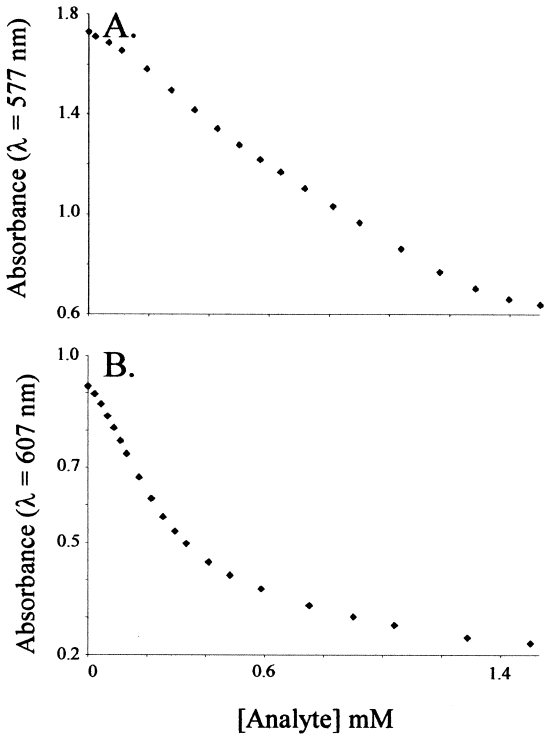

Figure 7. Calibration curves used for the citrate assay (5% (v/v) water in methanol with a 10 mM HEPES buffer at pH 7.5). (A) UV–Vis calibration curve using **4** as the indicator (55 μM **4**, 1.13 mM **1**, λ=577 nm). (B) UV–Vis calibration curve using **5** as the indicator (55 μm **5**, 1.13 mM **1**, λ=607 nm).

In order to demonstrate that these sensing systems can be employed for practical uses, calibration curves were generated for citrate (Fig. 7) in order to evaluate various citrus beverages. The determination of citrate in various beverages was performed by UV–Vis spectroscopy in 10 mM HEPES buffer at pH 7.5 with a 25% (v/v) water in methanol mixture.

For each assay utilizing a different indicator, aliquots ranging between 10 and 400 μL of each type of beverage were added to the sensing ensemble (1.00 mL). An absorbance reading was taken, and the citrate concentration was determined from the calibration curve. These values are reported in Table 1. The citrate concentrations determined for Sprite® and Snapple® Starfruit drink by each sensing system are in agreement within 10% of each other. The values calculated with the two citrate assays for Schweppes® tonic water differ by 13%. Based upon our previous results, we know that **1** is selective for citrate in these kinds of beverages, and this data shows that our new colorimetric competition method works well to quantitate citrate in a practical application.

Table 1. Concentration of citrate (mM) in beverages determined by different sensing systems. The reported values shown are the average value±the standard deviation of three measurements

	Concentration (mM)	
	4+**5**:**1**	**4**+**6**:**1**
Sprite	4.9±0.5	4.4±0.3
Snapple (Starfruit)	11±1	10±1
Tonic water (Schweppes)	13±2	11±3

3. Outlook

The competitive indicator method has been extended to systems containing both 1:1 and 1:2 molecular complexes. Such competition assays give a facile method of determining the concentration of a target analyte without introducing additional covalent structure in the synthetic receptor. In general, we predict that the use of complexometric dyes that have similar functionalities to that of the analyte of interest can be used to generate many different colorimetric competition assays. In conclusion, sophisticated hosts can be interfaced with different indicators to create sensing systems for the analysis of analytes in aqueous media.

4. Experimental

4.1. Materials

All the solvents used in spectrophotometric studies were of spectroscopic grade and purchased from Aldrich. Xylenol orange and methylthymol blue were obtained from Aldrich and used without further purification. Buffer components were of reagent grade. The synthesis of **1** has been previously reported.[7]

4.2. Absorption studies

The absorption spectra were recorded on a Beckman DU-640 UV–Vis spectrophotometer. All spectrophotometric measurements were done at a constant pH (7.5) in 10 mM HEPES at room temperature (25°C). Solutions were measured in a 1.00 cm (3 mL) quartz cuvette. The solvent system employed for all the titration experiments was a 25% (v/v) water in methanol mixture.

The first set of absorption titrations (adding **1** to **4** and **1** to **5**) were performed by keeping the concentration of the indicator constant (55 μM) while varying the concentration of **1**. Data obtained from these titrations were used in the determination of affinity constants for **1** to **4** and **1** to **5**. The second set of absorption titrations (adding **2** to **1/4** and **2** to **1/5**) were performed by keeping both the concentration of each indicator **4** and **5** (55 μM) and **1** (1.13 mM) constant, while varying the concentration of **2**. Data obtained from these titrations were used to generate calibration curves for citrate.

4.3. Extraction of binding constants

The binding constants of **1** to each indicator was determined from the data obtained from the two titration experiments described earlier. The absorbance was recorded at 577 nm for the addition of **1** to **4** assay and 607 nm for the addition of **1** to **5** assay. The binding constants were determined from the plot of ($\Delta A/b$) vs total citrate concentration using Eq. (1) where b=1.00 cm, [H_i] was found using Eq. (4), [I_T] is the total indicator concentration (55 μM), $\Delta\epsilon 1=\epsilon_{I/H}-\epsilon_I$ and $\Delta\epsilon_2=\epsilon_{I/H2}-\epsilon_I$. The values used for [$H_i$] were found by

solving Eq. (4) in Mathematica 3.0 for each $[H_T]$ known experimentally (0–1.4 mM) and initial estimates of K_1, K_2, $\Delta\epsilon_1$, and $\Delta\epsilon_2$. The values for $\Delta\epsilon_1$ and $\Delta\epsilon_2$ for the **1**+**4** assay were found to be 2.41×10^4 and $1.13\times10^4\ cm^{-1}\ M^{-1}$, respectively. The values for $\Delta\epsilon_1$ and $\Delta\epsilon_2$ for the **1**+**5** assay were found to be 2.75×10^4 and $8.19\times10^3\ cm^{-1}\ M^{-1}$, respectively.

4.4. Beverage analysis

For the UV–Vis citrate assay, sample preparation was dependent on the beverage being analyzed. The tonic water and Sprite® samples were sonicated and the pH of each sample was then adjusted to 7.5 with aqueous sodium hydroxide. The Snapple® fruit drink was filtered. This solution was then brought to a pH of 7.5 with additions of aqueous sodium hydroxide.

An aliquot (25.0 mL) of each beverage sample was lyophilized to remove the water. The residue was then re-dissolved in 25% (v/v) water in methanol (10.0 mL). An aliquot (300 μL) of this beverage solution was added to the sensing ensemble (55 μM **4** or **5** and 1.13 mM **1**) and brought to a total volume of 2.00 mL. Then subsequent portions of this solution (10–200 μL) were added to the sensing ensemble (1.00 mL). An absorbance value was recorded for each addition and the corresponding citrate concentration value was obtained from the calibration curve (Fig. 7). The final values reported in Table 1 were obtained by multiplying the value determined from the calibration curve by the dilution factor.

Appendix A

The system studied contained 1:1 (I:H) and 1:2 ($I:H_2$) complexes of indicator (I) with host (H). The following Eqs. (A1) and (A2) describe the interactions between host (**1**) and indicator (**4** or **5**).

$$I + H \rightleftharpoons IH \tag{A1}$$

$$IH + H \rightleftharpoons IH_2 \tag{A2}$$

The absorbance of the solution of xylenol orange (A_o) prior to the addition of host is described by Beer's Law, Eq. (A3).

$$A_o = \epsilon b[I] \tag{A3}$$

where ϵ is the molar absorptivity of the indicator, b is the path length of light through the sample solution, and [I] is the concentration of the indicator present.

After the addition of host, the equation for describing all the absorbing species (A) in the solution becomes:

$$A = \epsilon_I b[I_i] + \epsilon_H b[H_i] + \epsilon_{IH} b[IH] + \epsilon_{IH2} b[IH_2] \tag{A4}$$

where $[I_i]$ and $[H_i]$ represent the concentration of the free indicator and host in solution, respectively, and [IH] and $[IH_2]$ are the concentrations of any complexes that may form between the them.

The total concentration of each species (I_T and H_T) is depicted by the mass balance equations for both the indicator and the host molecule.

$$[I_T] = [I_i] + [IH] + [IH_2] \tag{A5}$$

$$[H_T] = [H_i] + [IH] + 2[IH_2] \tag{A6}$$

Solving Eqs. (A5) and (A6) for $[I_i]$ and $[H_i]$, respectively and incorporating the expressions into Eq. (A4) gives Eq. (A7).

$$A = \epsilon_I b([I_T] - [IH] - [IH_2]) + \epsilon_H b([H_T] - [IH] - 2[IH_2]) + \epsilon_{IH} b[IH] + \epsilon_{IH2} b[IH_2] \tag{A7}$$

Since the host has no absorbance at the wavelength that is being monitored, the ϵ_H term becomes zero. Once eliminating this term and combining like terms, the equation becomes:

$$A = \epsilon_I b[I_T] + (\epsilon_{IH} - \epsilon_I) b[IH] + (\epsilon_{IH2} - \epsilon_I) b[IH_2] \tag{A8}$$

Dividing the path length from each side of the equation gives:

$$\frac{A}{b} = \epsilon_I[I_T] + \Delta\epsilon_1[IH] + \Delta\epsilon_2[IH_2] \tag{A9}$$

where $\Delta\epsilon_1 = \epsilon_{IH} - \epsilon_I$ and $\Delta\epsilon_2 = \epsilon_{IH2} - \epsilon_I$. The equilibrium constants in this system are given by:

$$K_1 = \frac{[IH]}{[H_i][I_i]} \tag{A10}$$

$$K_2 = \frac{[IH_2]}{[IH][H_i]} \tag{A11}$$

Rearrangement of these expressions and substitution into Eq. (A9) gives the result:

$$\frac{A}{b} = \epsilon_I[I_T] + \Delta\epsilon_1(K_1[H_i][I_i]) + \Delta\epsilon_2\left(K_2K_1[H_i]^2[I_i]\right) \tag{A12}$$

Since $[I_T]$ is held constant, the absorbance of the indicator prior to the first addition of host (A_0) is subtracted from each subsequent absorbance reading after the addition of the host (A_i). This results leads to the ϵ_I term dropping out of the expression.

$$\frac{\Delta A}{b} = \Delta\epsilon_1(K_1[H_i][I_i]) + \Delta\epsilon_2\left(K_2K_1[H_i]^2[I_i]\right) \tag{A13}$$

As mentioned earlier, the equilibrium expressions can be rewritten as:

$$[IH] = K_1[H_i][I_i] \tag{A14}$$

$$[IH_2] = K_2[H_i]^2[I_i] \tag{A15}$$

Using these values and substituting into the mass balance Eq. (A5) and solving for $[I_i]$ will give the equation:

$$[I_i] = \frac{[I_T]}{1 + K_1[H_i] + K_2K_1[H_i]^2} \tag{A16}$$

Combining Eq. (A16) with Eq. (A13) results in the equation for the binding isotherm for a 1:2 ($I:H_2$) complex.

$$\frac{\Delta A}{b} = \frac{(K_1[H_i][I_T])(\Delta\epsilon_1 + \Delta\epsilon_2K_2[H_i])}{1 + K_1[H_i] + K_2K_1[H_i]^2} \tag{A17}$$

The term $[H_T]$ is a value that can be determined experimentally. Where as, the concentration of free host, $[H_i]$, cannot be measured directly. This creates the need to relate $[H_i]$ to $[H_T]$ and can be accomplished by substituting Eq. (A16) into the rearranged form of Eq. (A14) giving Eq. (A18).

$$[IH] = \frac{K_1[H_i][I_T]}{1 + K_1[H_i] + K_2K_1[H_i]^2} \quad \text{(A18)}$$

Now, substitute Eq. (A18) into the mass balance equation for $[H_T]$. This relates the total concentration of host to the concentration of free host in solution.

$$[H_T] = [H_i] + \left(\frac{K_1[H_i][I_T]}{1 + K_1[H_i] + K_2K_1[H_i]^2}\right) + \left(\frac{2K_2K_1[I_T][H_i]^2}{1 + K_1[H_i] + K_2K_1[H_i]^2}\right) \quad \text{(A19)}$$

Rearrangement of Eq. (A19) in order to solve for $[H_i]$ gives the following cubic expression:

$$K_1K_2[H_i]^3 + K_1(2K_2[I_T] - K_2[H_T] + 1)[H_i]^2 + (K_1[I_T] - K_1[H_T] + 1)[H_i] - [H_T] = 0 \quad \text{(A20)}$$

Using Eqs. (A17) and (A20), it is possible to extract a binding constant from a plot of the change in absorbance (ΔA) versus the total concentration of indicator $[I_T]$. A discussion of how the actual process was performed is described in the text of this article.

References

1. (a) Yoon, J.; Czarnik, A. W. *J. Am. Chem. Soc.* **1992**, *114*, 5874–5875. (b) James, T. D.; Sandanayake Sanmankumara, K. R. A.; Shinkai, S. *Nature* **1995**, *374*, 345–347. (c) James, T. D.; Linnane, P.; Shinkai, S. *Chem. Commun.* **1996**, *3*, 281–288. (d) James, T. D.; Sandanayake Sanmankumara, K. R. A.; Shinkai, S. *Angew. Chem., Int. Ed. Engl.* **1996**, *35*, 1911–1922.
2. (a) Sousa, L. R.; Larson, J. M. *J. Am. Chem. Soc.* **1977**, *99*, 307–310. (b) Hong, S.-Y.; Czarnik, A. W. *J. Am. Chem. Soc.* **1993**, *115*, 3330–3331. (c) Lutengerg, R. J. W.; Brzozka, Z.; Casnati, A.; Ungaro, R.; Engbersen, J. F. J.; Reinhoudt, D. N. *Anal. Chim. Acta* **1995**, *310*, 263–267. (d) Prasanna de Silva, A.; Nimal Gunaratne, H. Q.; Gunnlaugsson, T.; Nieuwenhuizen, M. *Chem. Commun.* **1996**, 1967–1968. (e) Ungaro, R.; Arduini, A.; Casnati, A.; Pochini, A.; Ugozzoli, F. *Pure Appl. Chem.* **1996**, *68*, 1213–1218. (f) Pina, F.; Alexandra Bernardo, M.; García-España, E. *Eur. J. Inorg. Chem.* **2000**, *10*, 2143–2157.
3. (a) Schmidtchen, F. P.; Berger, M. *Chem. Rev.* **1997**, *97*, 1609–1646. (b) Antonisse, M. G.; Reinhoudt, D. N. *Chem. Commun.* **1998**, *4*, 443–448. (c) Beer, P. D.; Gale, P. A. *Angew. Chem., Int. Ed. Engl.* **2001**, *40*, 486–516.
4. (a) Prasanna de Silva, A. P.; Nimal Gunaratne, H. Q.; Gunnlaugsson, T.; Huxley, A. J. M.; McCoy, C. P.; Rademacher, J. T.; Rice, T. E. *Chem. Rev.* **1997**, *97*, 1515–1566. (b) Bourson, J.; Pouget, J.; Valeur, B. *J. Phys. Chem.* **1993**, *97*, 4552–4557. (c) Vance, D. H.; Czarnik, A. W. *J. Am. Chem. Soc.* **1994**, *116*, 9397–9398. (d) Czarnik, A. W. *Acc. Chem. Res.* **1994**, *27*, 302–308. (e) Fery-Forgues, S.; Le Bris, M.-T.; Guetté, J.-P.; Valeur, B. *J. Phys. Chem.* **1988**, *92*, 6233–6237.
5. Stryer, L. *Biochemistry*; Freeman: New York, 1995; p 61.
6. (a) Muñoz de la Peña, A.; Ndou, T.; Zung, J. B.; Warner, I. M. *J. Phys. Chem.* **1991**, *95*, 3330–3334. (b) Connors, K. A. *Binding Constants: The Measurement of Molecular Complex Stability*; Wiley: New York, 1987; p 161. (c) Pendergast, D. D.; Connors, K. A. *J. Pharm. Sci.* **1984**, *73*, 1779–1783. (d) Rossotti, F. J. C.; Rossotti, H. S. *The Determination of Stability Constants*; McGraw-Hill: New York, 1961; p 108. (e) Lenkinski, R. E.; Elgavish, G. A.; Reuben, J. *J. Magn. Reson.* **1978**, *32*, 367–376.
7. Metzger, A.; Lynch, V. M.; Anslyn, E. V. *Angew. Chem., Int. Ed. Engl.* **1997**, *36*, 862–865.
8. Metzger, A.; Anslyn, E. V. *Angew. Chem., Int. Ed. Engl.* **1998**, *37*, 649–652.
9. (a) Niikura, K.; Metzger, A.; Anslyn, E. V. *J. Am. Chem. Soc.* **1998**, *120*, 8533–8534. (b) Lavigne, J. J.; Anslyn, E. V. *Angew. Chem., Int. Ed. Engl.* **1999**, *38*, 3666–3669. (c) Cabell, L. A.; Monahan, M. K.; Anslyn, E. V. *Tetrahedron Lett.* **1999**, *40*, 7753–7756.
10. Kilway, K. V.; Seigel, J. S. *J. Am. Chem. Soc.* **1995**, *114*, 255–261.
11. Schnieder, S. E.; O'Niel, S. N.; Anslyn, E. V. *J. Am. Chem. Soc.* **2000**, *122*, 542–543.
12. (a) Seok Oh, K.; Lee, C.-W.; Choi, H. S.; Lee, S. J.; Kim, L. S. *Org. Lett.* **2000**, *2*, 2679–2681. (b) Chin, J.; Walsdorff, C.; Stranix, B.; Oh, J.; Chung, H. J.; Park, S.-M.; Kim, K. *Angew Chem., Int. Ed. Engl.* **1999**, *38*, 2756–2759. (c) Szabo, T.; O'Leary, B. M.; Rebek, J. *Angew. Chem., Int. Ed. Engl.* **1998**, *37*, 3410–3413.
13. (a) Müller, G.; Riede, J.; Schmidtchen, F. P. *Angew. Chem., Int. Ed. Engl.* **1988**, *27*, 1516–1518. (b) Echavarren, A.; Galán, A.; Lehn, J. M. *J. Am. Chem. Soc.* **1989**, *111*, 4994–4995.
14. Benesi, H. A.; Hildebrand, J. H. *J. Am. Chem. Soc.* **1949**, *71*, 2703–2707.
15. (a) Grell, E.; Bremer, C. *Inorg. Chim. Acta* **1996**, *241*, 13–19. (b) Green, F. J. *The Sigma-Aldrich Handbook of Stains, Dyes and Indicators*; Aldrich Chemical Company: Milwaukee, 1990; p 468 and 740. (c) Hulanicki, A.; Glab, S.; Ackermann, G. *Pure Appl. Chem.* **1983**, *55*, 1137–1230. (d) Wardi, A. H.; Allen, W. S.; Varma, R. *Anal. Chem.* **1974**, *46*, 919–920.
16. Kneeland, D. M.; Ariga, K.; Lynch, V. M.; Huang, C.-Y.; Anslyn, E. V. *J. Am. Chem. Soc.* **1993**, *115*, 10042–10055.